

Estimation of the isotope effect on the lattice thermal conductivity of group IV and group III-V semiconductors

D. T. Morelli* and J. P. Heremans

Delphi Research Labs, Shelby Township, Michigan 48315

G. A. Slack

Rensselaer Polytechnic Institute, Troy, New York 12180

(Received 17 July 2002; published 1 November 2002)

The isotope effect on the lattice thermal conductivity for group IV and group III-V semiconductors is calculated using the Debye-Callaway model modified to include both transverse and longitudinal phonon modes explicitly. The frequency and temperature dependences of the normal and umklapp phonon-scattering rates are kept the same for all compounds. The model requires as adjustable parameters only the longitudinal and transverse phonon Grüneisen constants and the effective sample diameter. The model can quantitatively account for the observed isotope effect in diamond and germanium but not in silicon. The magnitude of the isotope effect is predicted for silicon carbide, boron nitride, and gallium nitride. In the case of boron nitride the predicted increase in the room-temperature thermal conductivity with isotopic enrichment is in excess of 100%. Finally, a more general method of estimating normal phonon-scattering rate coefficients for other types of solids is presented.

DOI: 10.1103/PhysRevB.66.195304

PACS number(s): 66.70.+f, 63.20.Kr

INTRODUCTION

The thermal conductivity, κ , of almost all pure electrically insulating crystals has a universal behavior as a function of temperature: starting just below the melting point, the thermal conductivity increases as T^{-1} or faster with decreasing temperature, reaches a maximum at $\approx 0.05\theta_D$, where θ_D is the Debye temperature of the crystal, and falls off as T^3 at lower temperatures. The high-temperature behavior is due to scattering of phonons amongst themselves via umklapp processes. The probability of these processes occurring falls off exponentially with decreasing temperature, causing the phonon mean free path and the thermal conductivity to rise. Finally, when the phonon mean free path becomes on the order of the dimensions of the crystal, the thermal conductivity falls again, mirroring the temperature dependence of the specific heat. Any impurities or imperfections in the crystal will also scatter phonons and decrease the thermal conductivity. This latter effect is particularly noticeable at the peak in the thermal conductivity, where phonon-phonon umklapp processes and boundary scattering are both present but weak. Since the early work of Pomeranchuk¹ it has been known that isotopes, due to their mass difference, can scatter phonons and decrease the thermal conductivity. This effect was discussed also by Slack.² Geballe and Hull³ provided unequivocal evidence for the influence of isotopes on the thermal conductivity with their experiments on natural abundance and isotopically purified germanium.

With the ready availability of isotopically purified source materials, the isotope effect has undergone reexamination over the last decade. Isotopically purified diamond⁴⁻⁷ displays a room-temperature isotope effect on the order of 40% at room temperature. In a very thorough investigation of the isotope effect in germanium, Asen-Palmer *et al.*⁸ showed that an isotopically purified sample had κ 30% larger compared to natural abundance Ge. Very recently, Ruf *et al.*⁹ reported

an isotope effect in silicon of 60% at 300 K. The magnitude of this last effect is significant because, if confirmed, it could prove technologically useful in the thermal management of silicon-based power electronics systems.

The magnitude of the isotope effect in these materials is at first surprising since a simple estimate using standard Debye theory of lattice thermal conductivity¹⁰ yields increases in all cases of 5% or less. A more thorough and complete understanding of the isotope effect in these materials must recognize the importance of normal phonon-phonon scattering processes.¹¹⁻¹³ These scattering processes, which were considered many years ago by Callaway,¹⁴ do not themselves contribute directly to the thermal resistance, but result in a redistribution of momentum and energy amongst phonons more likely to undergo umklapp scattering. In the case of diamond, it has been argued¹¹⁻¹³ that the effect is of the right order of magnitude to explain the experimental result, although assuming infinitely rapid normal processes can only qualitatively fit the data.⁶

For the case of germanium, the analysis of Asen-Palmer⁸ modified the Debye-Callaway model by treating the contributions of longitudinal and transverse phonons explicitly. This approach fixed the boundary and isotope scattering rates using the known values of the crystal dimensions and isotope content, respectively, and fit the data using six adjustable parameters: the four coefficients for normal and umklapp scattering for the transverse and longitudinal modes, respectively, and the two umklapp scattering exponents. A similar approach was adopted by Ruf *et al.*⁹ for the case of silicon. While these models give very satisfactory fits to the experimental data, there is no justification given for the magnitude of the phonon-scattering coefficients. For instance, the coefficient for umklapp scattering of longitudinal phonons in Ge is chosen to be five times that for transverse phonons, whereas on the basis of the simple model of Leibfried and Schlömann¹⁵ one would expect the opposite to be the case.

The purpose of the present paper is to model the lattice thermal conductivity and isotope effect in Ge, Si, and diamond using an approach similar to that of Asen-Palmer *et al.*,⁸ but employing phonon-scattering rates calculated from a simple model and using parameters derived from known phonon-dispersion relations for these crystals. Using this approach, we can fit the experimental data for both natural abundance and isotopically purified germanium and diamond, and for natural abundance silicon. The recent results of Ruf *et al.*⁹ on isotopically enriched silicon are not consistent with the model, however. The latter experimental results must be considered anomalous, as they exhibit a factor of 4 larger thermal conductivity of the isotopically enriched sample in the boundary scattering regime, in spite of the fact that the crystal dimensions are nearly the same. Additionally the results of Ruf *et al.* indicate an enhancement in the thermal conductivity of the isotopically enriched sample over natural abundance silicon of roughly 60% that is essentially independent of temperature up to 400 K, a behavior qualitatively different from that in germanium and diamond. Finally, we use the model developed here to estimate the isotope effect on the lattice thermal conductivity of silicon carbide, boron nitride, and gallium nitride.

MODIFIED DEBYE-CALLAWAY MODEL OF LATTICE THERMAL CONDUCTIVITY

Following the approach used by Asen-Palmer,⁸ we calculate the lattice thermal conductivity using the Debye-Callaway formalism and sum over one longitudinal (κ_L) and two degenerate transverse (κ_T) phonon branches:

$$\kappa = \kappa_L + 2\kappa_T, \quad (1)$$

where

$$\kappa_L = \kappa_{L1} + \kappa_{L2}. \quad (2)$$

The partial conductivities κ_{L1} and κ_{L2} are the usual Debye-Callaway terms given by

$$\kappa_{L1} = \frac{1}{3} C_L T^3 \int_0^{\theta_L/T} \frac{\tau_C^L(x) x^4 e^x}{(e^x - 1)^2} dx, \quad (3a)$$

$$\kappa_{L2} = \frac{1}{3} C_L T^3 \frac{\left[\int_0^{\theta_L/T} \frac{\tau_C^L(x) x^4 e^x}{\tau_N(x)(e^x - 1)^2} dx \right]^2}{\int_0^{\theta_L/T} \frac{\tau_C^L(x) x^4 e^x}{\tau_N^L(x) \tau_R^L(x)(e^x - 1)^2} dx}, \quad (3b)$$

and similarly, for the transverse phonons,

$$\kappa_{T1} = \frac{1}{3} C_T T^3 \int_0^{\theta_T/T} \frac{\tau_C^T(x) x^4 e^x}{(e^x - 1)^2} dx, \quad (4a)$$

$$\kappa_{T2} = \frac{1}{3} C_T T^3 \frac{\left[\int_0^{\theta_T/T} \frac{\tau_C^T(x) x^4 e^x}{\tau_N^T(x)(e^x - 1)^2} dx \right]^2}{\int_0^{\theta_T/T} \frac{\tau_C^T(x) x^4 e^x}{\tau_N^T(x) \tau_R^T(x)(e^x - 1)^2} dx}. \quad (4b)$$

In these expressions, $(\tau_N)^{-1}$ is the scattering rate for normal phonon processes, $(\tau_R)^{-1}$ is the sum of all resistive scattering processes, and $(\tau_C)^{-1} = (\tau_N)^{-1} + (\tau_R)^{-1}$, with superscripts L and T denoting longitudinal and transverse phonons, respectively. The quantities θ_L and θ_T are Debye temperatures appropriate for the longitudinal and transverse phonon branches, respectively, and

$$C_{L(T)} = \frac{k_B^4}{2\pi^2 \hbar^3 \nu_{L(T)}} \quad (5)$$

and

$$x = \frac{\hbar \omega}{k_B T}. \quad (6)$$

Here \hbar is the Planck constant, k_B is the Boltzmann constant, ω is the phonon frequency, and $\nu_{L(T)}$ are the longitudinal (transverse) acoustic phonon velocities, respectively.

The temperature dependence and the magnitude of the lattice thermal conductivity calculated using the Callaway model are dependent on the temperature and frequency dependence of the scattering rates comprising $(\tau_N)^{-1}$ and $(\tau_R)^{-1}$, their coefficients, and the Debye temperatures and phonon velocities. Thus extreme care must be exercised when selecting these parameters. In the following section, we discuss our process for making these selections for the types of crystals considered here.

PHONON-SCATTERING RATES AND DEBYE TEMPERATURES FOR GROUPS IV AND III-V SEMICONDUCTORS

For pure single crystals, we assume that the resistive scattering rate is the sum of scattering rates due to phonon-phonon umklapp scattering, point defect scattering due to the presence of isotopes of different mass, and scattering from the boundaries of the crystal:

$$(\tau_R^L)^{-1} = (\tau_U^L)^{-1} + (\tau_I^L)^{-1} + (\tau_B^L)^{-1} \quad (7)$$

and

$$(\tau_R^T)^{-1} = (\tau_U^T)^{-1} + (\tau_I^T)^{-1} + (\tau_B^T)^{-1}. \quad (8)$$

In this approach, unlike that of Asen-Palmer,⁸ the isotope and boundary scattering, as well as the umklapp scattering, depend on phonon mode, as should be the case since each of the former rates depends on the phonon velocities, which are different for each mode. We now discuss the forms of these scattering rates.

Phonon-phonon umklapp scattering

That phonon-phonon umklapp processes should give rise to an exponential behavior of the lattice thermal conductivity at high temperatures was proposed long ago by Peierls¹⁶ who suggested the form $\kappa \propto T^n \exp(\theta/bT)$ with n and b on the order of unity. On the basis of the model of Leibfried and Schlömann¹⁵ and comparing the thermal conductivity of several pure crystals, Slack and Galginitis¹⁷ suggested the fol-

TABLE I. Zone-boundary frequencies $f_{T,L}$ of transverse and longitudinal phonons, respectively, for germanium (Ref. 34), silicon (Ref. 35), diamond (Ref. 36), silicon carbide (Ref. 37), boron nitride (Ref. 38), and gallium nitride (Ref. 39), θ_T and θ_L are Debye temperatures calculated from these frequencies. For comparison, we show θ_{Tv} and θ_{Lv} calculated from phonon velocities ν_T and ν_L using Eq. (13), and Debye temperature θ_{SH} determined from the specific heat.

Material	f_T (THz)	f_L (THz)	ν_T (m s ⁻¹)	ν_L (m s ⁻¹)	θ_T (K)	θ_L (K)	θ_{Tv} (K)	θ_{Lv} (K)	θ_{SH} (K)
Ge	3.1	6.9	3540	4920	150	333	371	516	374
Si	5.1	12.4	5840	8430	240	586	638	919	645
C	25.5	38.0	12 800	17 500	1233	1820	2138	2922	2220
SiC	11.0	18.9	8 840	12 430	524	900	946	1330	1185
BN	21	31	10 500	15 000	1003	1479	1376	1789	1750
GaN	~6.3 ^a	~9	4130	7 960	301	434	631	1010	650

^aAverage of two nondegenerate TA modes along Γ - M in the wurtzite structure Brillouin zone.

lowing form for the umklapp scattering rate for phonons of velocity ν and Grüneisen parameter γ .

$$\tau_U^{-1}(\omega) = B_U \omega^2 T e^{-\theta/3T} \quad (9)$$

with

$$B_U \approx \frac{\hbar \gamma^2}{M \nu^2 \theta}, \quad (10)$$

where M is the average mass of an atom in the crystal. They found that this expression could fit the thermal conductivity of several pure crystals above the maximum in the thermal conductivity to within 20%. Several other expressions using other values for n and b for the umklapp scattering rate have appeared in the literature.^{18–21} Clearly the values chosen are sensitive to other parameters used in the fit; for instance, choosing too high a value for the Debye temperature requires a larger value of b or a larger value of the coefficient B_U . Abeles²² also attempted to include normal processes, but that approach, in which the exponential behavior of umklapp processes is ignored, is suitable only for temperatures well above the Debye temperature. In view of the results of Slack and Galginitis, we choose here to fix the umklapp scattering rate for longitudinal and transverse phonons as (replacing ω with x)

$$[\tau_U^L(x)]^{-1} = B_U^L \left(\frac{k_B}{\hbar} \right)^2 x^2 T^3 e^{-\theta_L/3T} \quad (11a)$$

with

$$B_U^L = \frac{\hbar \gamma_L^2}{M \nu_L^2 \theta_L} \quad (11b)$$

and

$$[\tau_U^T(x)]^{-1} = B_U^T \left(\frac{k_B}{\hbar} \right)^2 x^2 T^3 e^{-\theta_T/3T} \quad (12a)$$

with

$$B_U^T \approx \frac{\hbar \gamma_T^2}{M \nu_T^2 \theta_T}. \quad (12b)$$

The umklapp scattering rate thus depends on the transverse and longitudinal Debye temperature, phonon velocities, and Grüneisen parameters and, as such, will be different for different phonon modes. Since it is assumed that heat is carried only by acoustic phonons, we must be careful to choose the parameters corresponding only to these modes. This has been discussed in detail by Slack.²³ For instance, using a value of Debye temperature calculated from the specific heat at low temperatures (which for diamond is roughly 2200 K) clearly is not suitable, since this value would average in all phonon modes, both acoustic and optic, and would be too high an estimate for the acoustic modes only. Another approach would be to calculate the Debye temperature for each acoustic branch i from the acoustic-mode phonon velocity according to

$$\theta_i = \left(\frac{\theta \pi^2}{V} \right)^{1/3} \hbar \nu_i / k_B, \quad (13)$$

where V is the volume per atom. This has been done in the past for diamond.^{6,24} This again yields an overestimate of θ , because it neglects dispersion of the phonon branches near the zone boundary. Clearly we want to consider phonons of frequency only up to but not exceeding the maximum frequency ω_{\max} at the zone boundary. For the crystals considered here, these are available either from inelastic neutron-scattering experiments or lattice-dynamical calculations. Table I displays the zone-boundary frequencies and the Debye temperatures calculated from them. Also shown for comparison are the Debye temperatures determined from the phonon velocities and from the specific heat. The differences are quite large and obviously have affected the choice of parameters b and B_U in the umklapp scattering rate in previous analyses of the thermal conductivity.^{6,24}

The other piece of information we require to calculate our values of B_U are the mode Grüneisen parameters. The situation is problematic, because for some of the crystals considered here some of the mode Grüneisen parameters evolve from positive to negative values as the phonon wave vector moves outward from the zone center to the zone edge.²⁵ Generally speaking, the longitudinal modes have $\gamma \sim 0.9$ – 1.3 independent of frequency whereas the transverse

modes along $\langle 100 \rangle$ are in the range 0.3–1.0 for low frequency. In our model, we will use the longitudinal and transverse phonon Grüneisen constants as adjustable parameters.

Phonon-isotope scattering

Klemens²⁶ first provided the calculation of the scattering rate of phonons by isolated defects of mass different from that of the host in an otherwise perfect crystal. For the present cases of both longitudinal and transverse modes this scattering rate takes the form

$$[\tau_I^L(x)]^{-1} = \frac{Vk_B^4 \Gamma}{4\pi\hbar^4 \nu_L^3} x^4 T^4 \quad (14a)$$

and

$$[\tau_I^T(x)]^{-1} = \frac{Vk_B^4 \Gamma}{4\pi\hbar^4 \nu_T^3} x^4 T^4. \quad (14b)$$

Thus the scattering rate by isotopes also depends on the phonon mode through the phonon velocity. The mass-fluctuation phonon-scattering parameter Γ for a single element made up of several naturally occurring isotopes is

$$\Gamma = \sum_i c_i \left[\frac{m_i - \bar{m}}{\bar{m}} \right]^2 \quad (15a)$$

with

$$\bar{m} = \sum_i c_i m_i, \quad (15b)$$

where m_i is the atomic mass of the i th isotope and c_i is the fractional atomic natural abundance. The correct calculation of Γ for a binary compound AB composed of two different elements is given by²⁷

$$\Gamma(AB) = 2 \left[\left(\frac{M_A}{M_A + M_B} \right)^2 \Gamma(A) + \left(\frac{M_B}{M_A + M_B} \right)^2 \Gamma(B) \right], \quad (16)$$

where M_A is the average atomic mass of A and M_B is that of B . The factor of 2 in front of the square brackets is due to the fact that AB is a binary compound.²⁷ The values of Γ for several of the group IV and group III-V semiconductors considered here are given in Table II and are used to calculate the phonon-isotope scattering rates used in the model above.

Phonon-boundary scattering

The phonon-boundary scattering rate is assumed independent of temperature and frequency, and can be written as

$$(\tau_B^L)^{-1} = \frac{\nu_L}{d} \quad (17a)$$

and

$$(\tau_B^T)^{-1} = \frac{\nu_T}{d}, \quad (17b)$$

TABLE II. Natural isotope composition and associated scattering parameter Γ [Eqs. (15) and (16)] for several group III, IV, and V elements and group III-V semiconductors. The fourth and fifth columns display hypothetical isotopically disordered crystals and their associated scattering parameters, respectively.

Material	Natural isotope composition	$\Gamma (10^{-4})$	Disordered isotope composition	$\Gamma_{\text{dis}} (10^{-4})$
B	19.9% ¹⁰ B	13.5	50% ¹⁰ B	22.5
	80.1% ¹¹ B		50% ¹¹ B	
C	98.9% ¹² C	0.75	50% ¹² C	16.1
	1.1% ¹³ C		50% ¹³ C	
N	99.63% ¹⁴ N	0.19	50% ¹³ N	11.9
	0.37% ¹⁵ N		50% ¹⁵ N	
Si	92.2% ²⁸ Si	2.0	50% ²⁸ Si	11.8
	4.7% ²⁹ Si		50% ³⁰ Si	
	3.1% ³⁰ Si			
Ga	60.1% ⁶⁹ Ga	1.98	50% ⁶⁹ Ga	2.18
	39.9% ⁷¹ Ga		50% ⁷¹ Ga	
Ge	20.5% ⁷⁰ Ge	6.08	50% ⁷⁰ Ge	11.9
	27.4% ⁷² Ge		50% ⁷⁶ Ge	
	7.8% ⁷³ Ge			
	36.5% ⁷⁴ Ge			
	7.8% ⁷⁶ Ge			
SiC		2.09		14.5
BN		5.12		16.1
GaN		2.74		3.7

where d is the effective diameter of the sample. The value of d will be adjusted slightly for each crystal in order to fit the T^3 dependence of the thermal conductivity at the lowest temperatures.

Phonon-phonon normal scattering

Although normal phonon scattering is not a resistive process, the Callaway model requires knowledge of this scattering rate in order to calculate the thermal conductivity. Herring²⁸ has suggested several forms depending on the crystal class. For the present crystallographic class of materials, following the approach of Asen-Palmer,⁸ the appropriate forms for longitudinal and transverse phonons are

$$[\tau_N^L(\omega)]^{-1} = B_N^L \omega^2 T^3 \quad (18a)$$

and

$$[\tau_N^T(\omega)]^{-1} = B_N^T \omega T^4 \quad (18b)$$

or in terms of the dimensionless variable x ,

$$[\tau_N^L(x)]^{-1} = B_N^L \left(\frac{k_B}{\hbar} \right)^2 x^2 T^5 \quad (19a)$$

and

$$[\tau_N^T(x)]^{-1} = B_N^T \left(\frac{k_B}{\hbar} \right) x T^5. \quad (19b)$$

Little is known about the magnitudes B_N of the normal phonon-scattering rates. The usual approach is to simply use these quantities as adjustable parameters without regard to their dependence on the properties of a given crystal. Here we assert that these rates must be chosen to satisfy the following dependence on phonon velocity:²⁹

$$B_N^L \approx \frac{k_B^3 \gamma_L^2 V}{M \hbar^2 \nu_L^5} \quad (20a)$$

and

$$B_N^T \approx \frac{k_B^4 \gamma_T^2 V}{M \hbar^3 \nu_T^5}. \quad (20b)$$

For the time being, we will present these forms of the scattering rate coefficients without proof and consider them as empirical relations only. A more general case and further discussion is considered in the Appendix. Thus, in our approach, these parameters are only adjustable to the extent that the Grüneisen parameters (which are the same values used for the umklapp rate) are allowed to vary in order to fit the data. We shall see later that this assertion is justified by the resulting values for γ_T and γ_L that emerge from the fits.

The procedure thus is to fit the experimental data on natural abundance crystals using only the transverse and longitudinal phonon Grüneisen constants as adjustable parameters (aside from slight adjustment of the effective sample dimension d to fit the data at the lowest temperature). The effect of isotopic enrichment is then calculated by allowing Γ to assume its value appropriate for the purified form of each crystal.

RESULTS AND DISCUSSION

The model fits to the lattice thermal conductivity of natural abundance and isotopically purified germanium, natural abundance and isotopically purified silicon, natural abundance and isotopically purified diamond, and natural abundance SiC are shown in Figs. 1–4 respectively. The data for germanium are from Asen-Palmer *et al.*⁸ for isotopically pure Ge and Glassbrenner and Slack³⁰ for natural abundance Ge (the latter data extend the fitting range up to several hundred Kelvin). Those for isotopically pure silicon are from Ruf *et al.*,⁹ whereas we again use the data of Glassbrenner and Slack³⁰ for natural abundance Si since these extend up to ≈ 1000 K. The data for diamond are from Olson *et al.*⁶ and the data for SiC are from an ultrahigh purity single crystal measured in our laboratory. The values of γ_L and γ_T used to generate the fits and the resulting values of the umklapp and normal phonon-scattering rate coefficients are displayed in Table III as are the calculated and observed magnitudes of the isotope effect at 300 K for germanium, silicon, and diamond. The mode Grüneisen parameters as a function of phonon frequency for some of the crystals here have been calculated using *ab initio* lattice-dynamical models. These are shown in Fig. 5 for the cases of Si, diamond, and BN. Since the scattering cross section for phonon interaction goes as the average value $\langle \gamma^2 \rangle$, we have calculated $\sqrt{\langle \gamma^2 \rangle}$ from these curves; these values are shown in Table III. The agreement

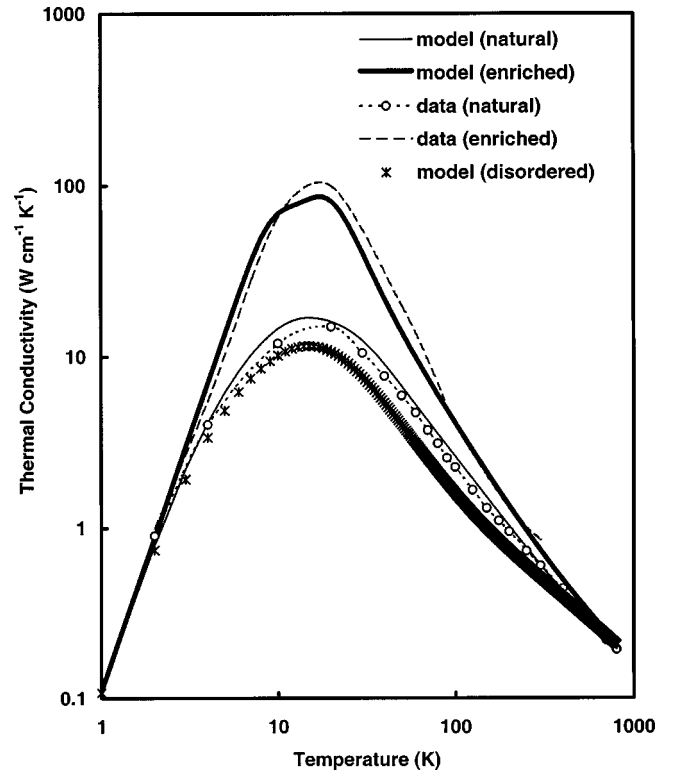


FIG. 1. Experimental data and model calculations of the thermal conductivity of natural abundance and isotopically pure germanium. Also shown is the model calculation of the thermal conductivity of an isotopically disordered Ge crystal whose composition is given in Table II.

between these values and those found from the fit to the thermal conductivity is quite good. Clearly the Grüneisen parameters for these crystals deviate significantly from the nominal value of $\gamma=2$ chosen many times to describe anharmonicity effects on the thermal conductivity.

We see that the model calculations can account quite well for both the magnitude and temperature dependence of the thermal conductivity as well as the magnitude of the isotope effect in germanium and diamond. In the case of silicon, the magnitude of the isotope effect at room temperature reported in Ref. 8 is much larger than that predicted by the model. As can be seen in Table III the experimental data reported for the isotopically purified silicon sample below 10 K require an anomalously large value of effective sample diameter d . This is possible if there is significant specular reflection from the surfaces of the sample. However, both the natural abundance and isotopically purified silicon specimens were grown and handled in the same way and presumably have similar surface conditions.⁹ It is not known why a reduction in isotope concentration would influence the nature of scattering deep into the boundary scattering regime. Further, the model neither predicts the observed 60% isotope effect in silicon at room temperature nor its near temperature independence from 100–400 K. This situation is quite unlike that for germanium and diamond for which the fit is able to reproduce quite well the magnitude and temperature dependence of both natural abundance and isotopically purified samples. It has been suggested³¹ that isotopically purified silicon with

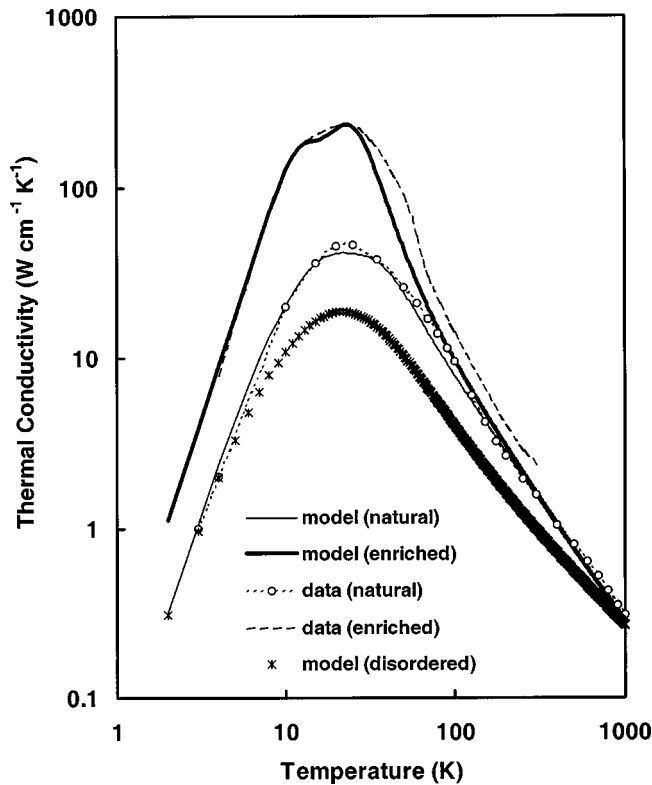


FIG. 2. Experimental data and model calculations of the thermal conductivity of natural abundance and isotopically pure silicon. Also shown is the model calculation of the thermal conductivity of an isotopically disordered Si crystal whose composition is given in Table II.

enhanced thermal conductivity may find use in improved thermal management of high-power silicon-based microelectronics. Further experimental investigation of the isotope effect in silicon would be desirable in order to confirm this effect.

Using the average values $\gamma_T=1.1$ and $\gamma_L=0.7$, we can estimate the strength of the normal phonon-scattering rate for gallium nitride and boron nitride and thus estimate the thermal conductivity. The results are shown in Figs. 6 and 7, respectively. The data for GaN are for a high-purity single crystal. We see that the model can account well for both the magnitude and the temperature dependence of the thermal conductivity of GaN. The model predicts an isotope effect of 5% in gallium nitride and greater than 100% in boron nitride. The latter effect is quite large due to the large isotope scattering parameter of boron, which is, in turn, due to both the small atomic number of boron and the abundance of two different isotopes of this element.

To estimate the degree to which the thermal conductivity of these semiconductors can be *reduced* using isotopic disorder, we have calculated the thermal conductivity for isotopic compositions at or near the maximum amount of disorder; see Table II. The results are shown in Figures 1–4, 6, and 7. We see that significant further reduction of the room-temperature thermal conductivity below that for the natural abundance of isotopes is possible in silicon, diamond, silicon carbide, and boron nitride. The thermal conductivity reduc-

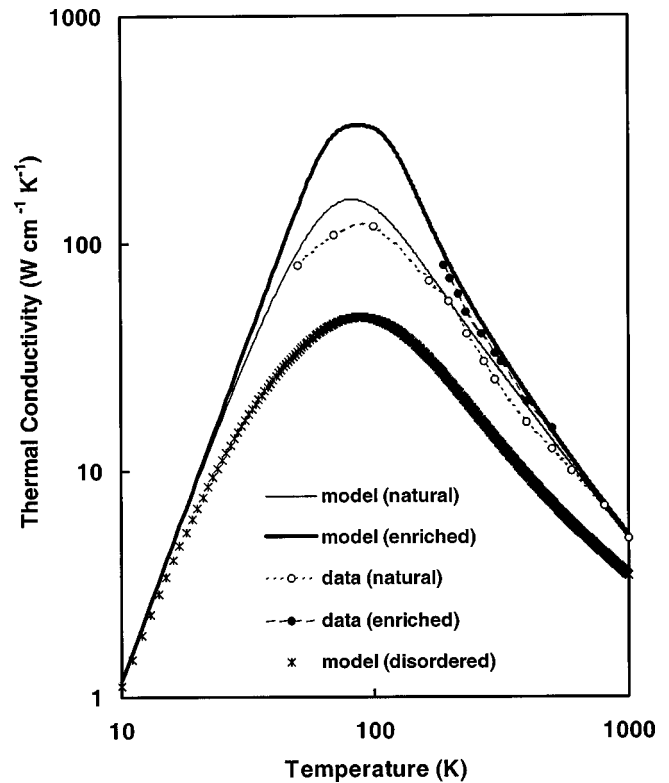


FIG. 3. Experimental data and model calculations of the thermal conductivity of natural abundance and isotopically pure diamond. Also shown is the model calculation of the thermal conductivity of an isotopically disordered diamond crystal whose composition is given in Table II.

tion in germanium and gallium nitride for natural abundance of isotopes in these semiconductors is already close to maximum reduction achievable using isotope scattering.

SUMMARY

A Debye-Callaway model modified to include both longitudinal and transverse phonon modes explicitly has been developed to describe the lattice thermal conductivity and isotope effect in diamond, silicon, and germanium. The model uses umklapp and normal phonon-scattering parameters that scale in a consistent manner with Debye temperature and phonon velocity. The calculated magnitude of the isotope effect is in good agreement with experiment for diamond and germanium, but not for silicon. Finally, the magnitude of the isotope effect has been estimated for gallium nitride, silicon carbide, and boron nitride. The method used here also provides a simple guide for estimating the magnitudes of the normal and umklapp phonon-scattering rates given the dispersion relations and mode Grüneisen parameters.

APPENDIX: OTHER FORMS OF THE NORMAL PHONON-SCATTERING RATE AND THEIR APPLICATION TO LITHIUM FLUORIDE AND SOLID NEON

In the treatment of Herring,²⁷ the normal phonon-scattering rate is written as

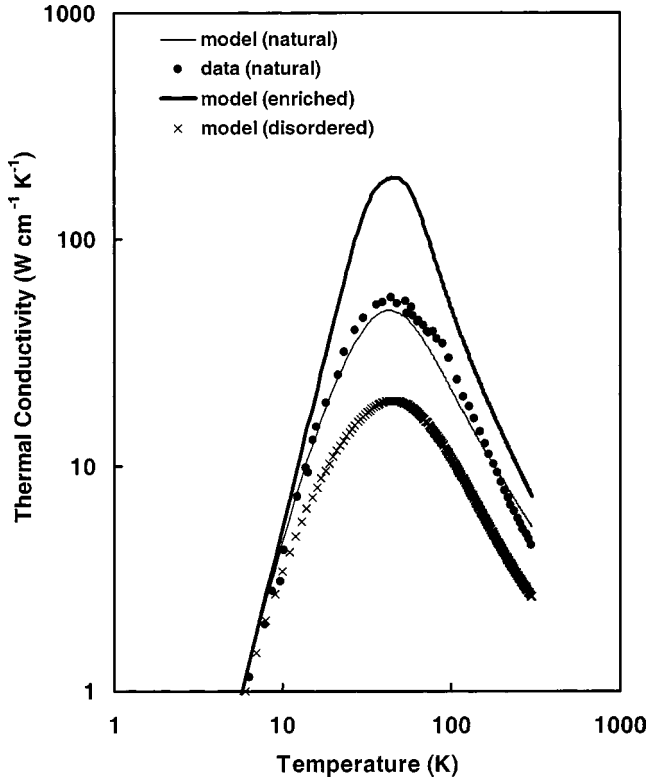


FIG. 4. Experimental data for the thermal conductivity of natural abundance silicon carbide and model calculations of the thermal conductivity of natural abundance and isotopically pure crystals. Also shown is the model calculation of the thermal conductivity of an isotopically disordered SiC crystal whose composition is given in Table II.

$$[\tau_N^L(\omega)]^{-1} = B_N \omega^a T^b. \quad (21)$$

We have considered the cases $(a,b)=(1,4)$ and $(a,b)=(2,3)$ above and have shown that the following equations give a good description of the coefficient:

$$B_N(1,4) = \frac{k_B^4 \gamma_T^2 V}{M \hbar^3 \nu^5} \quad (22a)$$

and

$$B_N(2,3) = \frac{k_B^3 \gamma_T^3 V}{M \hbar^2 \nu^5}, \quad (22b)$$

where ν is the phonon velocity. Another form of the normal scattering rate often employed to fit experimental data is

$$[\tau_N^L(\omega)]^{-1} = B_N \omega T^3, \quad (23)$$

for which the corresponding coefficient would take the form

$$B_N(1,3) \approx \frac{k_B^3 \gamma^2 V^{2/3}}{M \hbar^2 \nu^4}, \quad (24)$$

Equation (23) has been used by Novikov *et al.*¹³ to fit the thermal conductivity of diamond for which they find $B_N(1,3) = 4.4 \times 10^{-11} \text{ K}^{-3}$. Using $\gamma = 1.1$ and $\nu = 1.28 \times 10^4 \text{ m s}^{-1}$ in Eq. (24) we calculate $B_N(1,3) = 1.7 \times 10^{-11} \text{ K}^{-3}$.

Another case where Eq. (23) was used in a Debye-Callaway fit to the thermal conductivity is LiF.²⁰ In this case, the authors found $B_N(1,3) = 2.7 \times 10^{-10} \text{ K}^{-3}$. Using $V = 1.01 \times 10^{-30} \text{ m}^{-3}$, $\gamma = 1.5$,³² and $\nu = 5.3 \times 10^3 \text{ m s}^{-1}$ as the appropriate average sound velocity in LiF,³³ we find $B_N(1,3) = 3.1 \times 10^{-10} \text{ K}^{-3}$, again in quite good agreement with the fitted value.

For different values of a and b the normal phonon-scattering rate coefficient may be expressed as

$$B_N(a,b) \approx \left(\frac{k_B}{\hbar} \right)^b \frac{\hbar \gamma^2 V^{(a+b-2)/3}}{M \nu^{a+b}}. \quad (25)$$

This form for the normal phonon-scattering rate is similar to that for umklapp processes, Eq. (12), except that the dependence on Debye temperature is replaced by dependence on phonon velocity. This reflects the fact that normal processes involve mostly phonons with low wave vector for which dispersion at the zone boundary is unimportant.

As a final example, Kimber and Rogers²¹ used the Callaway model to interpret the thermal conductivity of isotopic

TABLE III. Values of Grüneisen parameters used in the fits of the thermal conductivity, and calculated values of the umklapp normal phonon-scattering rate coefficients for longitudinal and transverse phonons. λ_L' and γ_T' are the average values of the Grüneisen parameters calculated from lattice-dynamical calculations as described in the text. d is the effective sample diameter [Eqs. (17a) and (17b)] used in the fits. The last two columns show the measured and calculated increase in room-temperature thermal conductivity upon isotope enrichment.

Material	γ_L	γ_T	γ_L'	γ_T'	$(B_U)^T$ ($\text{s}^{-1} \text{ K}^{-3}$)	$(B_U)^L$ ($\text{s}^{-1} \text{ K}^{-3}$)	$(B_N)^T$ ($\text{s}^{-1} \text{ K}^{-5}$)	$(B_N)^L$ ($\text{s}^{-1} \text{ K}^{-5}$)	d (10^{-3} m)	$\Delta \kappa / \kappa_{\text{natural}}$ (%)	
										Expt.	Model
Ge	1.1	0.6			1.6×10^{-19}	1.3×10^{-19}	3.7×10^{-12}	1.9×10^{-23}	4	30	28
Si	1.1	0.6	1.04	0.56	1.0×10^{-19}	5.5×10^{-20}	7.1×10^{-13}	2.4×10^{-24}	4 (natural) 14 (enriched)	60	12
C	1.0	0.9	0.91	0.73	2.7×10^{-20}	9.6×10^{-21}	2.5×10^{-14}	4.1×10^{-26}	0.55	35	23
SiC	1.0	0.7			3.7×10^{-20}	2.3×10^{-20}	1.7×10^{-13}	4.8×10^{-25}	1		36
BN	1.0	0.7	0.94	0.74	2.2×10^{-20}	1.5×10^{-20}	5.7×10^{-14}	1.5×10^{-25}	1		125
GaN	1.0	0.7			1.1×10^{-19}	5.5×10^{-20}	1.5×10^{-12}	1.2×10^{-24}	0.8		5

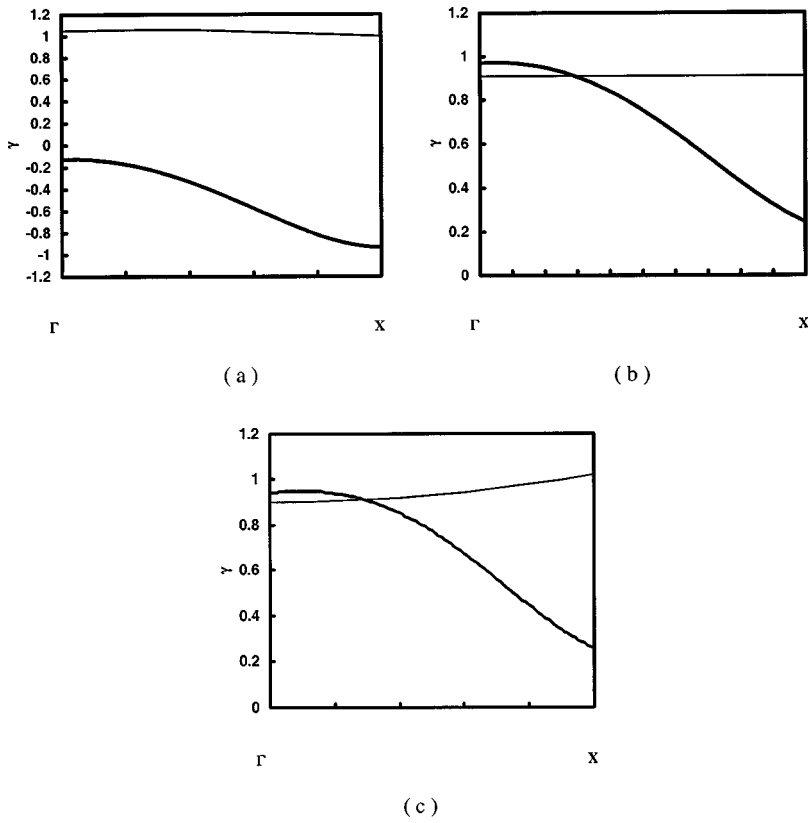


FIG. 5. Mode Grüneisen parameters along $\langle 100 \rangle$ from lattice-dynamical calculations for (a) silicon, (b) diamond, and (c) boron nitride. Light lines are longitudinal-acoustic modes and bold lines are transverse-acoustic modes.

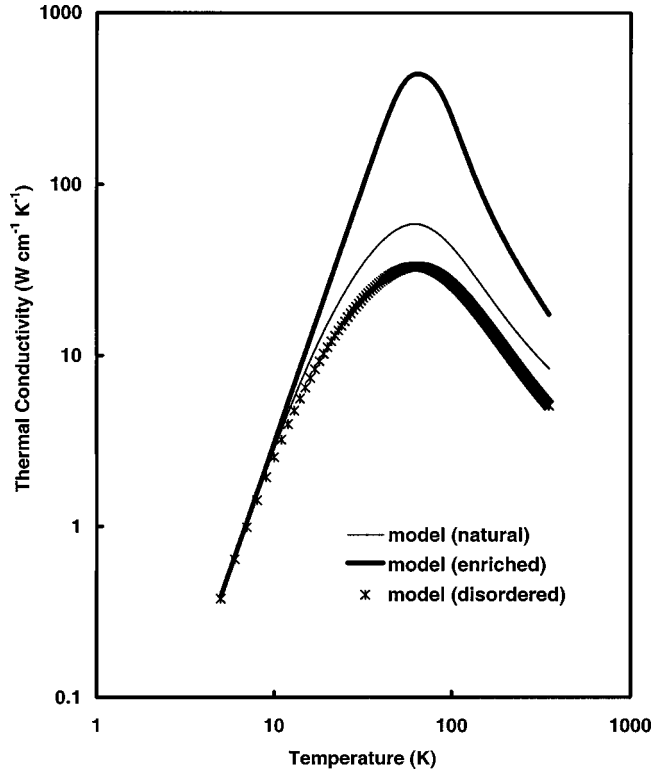


FIG. 6. Model calculations of the thermal conductivity of natural abundance and isotopically pure boron nitride. Also shown is the model calculation of the thermal conductivity of an isotopically disordered BN crystal whose composition is given in Table II.

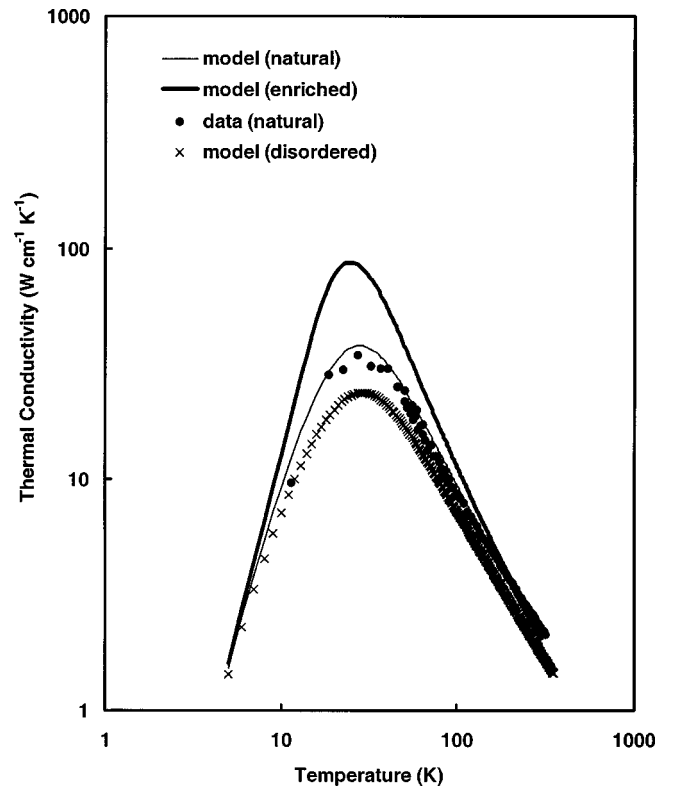


FIG. 7. Model calculations of the thermal conductivity of natural abundance and isotopically pure gallium nitride, and data on a natural abundance single crystal. Also shown is the model calculation of the thermal conductivity of an isotopically disordered GaN crystal whose composition is given in Table II.

mixtures of solid neon using a normal phonon-scattering rate of

$$\tau_N^{-1} = B_N \omega^2 T^2 \quad (26)$$

with $B_N = 2.6 \times 10^{-17} \text{ s K}^{-2}$. This corresponds to the case $(a, b) = (2, 2)$ for which Eq. (25) yields

$$B_N(2,2) m F \left(\frac{k_B}{\hbar} \right)^2 \frac{\hbar \gamma^2 V^{2/3}}{M \nu^4}. \quad (27)$$

Using $\gamma = 2$, $V = 2.29 \times 10^{-29} \text{ m}^3$, and $\nu = 718 \text{ m s}^{-1}$ appropriate for solid neon, this yields $B_N = 6.5 \times 10^{-17} \text{ s K}^{-2}$.

While the form (25) for the normal scattering rate coefficient must be considered as empirical only, we have seen that it can give a very good description of the magnitude of this rate as determined by fits to experimental data for a variety of materials with widely differing Debye temperatures. Thus, it can be used as a general guide for determining the strength of normal phonon scattering in crystals.

*Corresponding author. Email address:

donald.t.morelli@delphiauto.com

¹I. Pomeranchuk, J. Phys. (Moscow) **4**, 259 (1941).

²G. A. Slack, Phys. Rev. **105**, 829 (1957).

³T. H. Geballe and G. W. Hull, Phys. Rev. **110**, 773 (1958).

⁴D. G. Onn, A. Witek, Y. Z. Qiu, T. R. Anthony, and W. F. Banholzer, Phys. Rev. Lett. **68**, 2806 (1992).

⁵T. R. Anthony, W. F. Banholzer, J. F. Fleischer, L. Wei, P. K. Kuo, R. L. Thomas, and R. W. Pryor, Phys. Rev. B **42**, 1104 (1990).

⁶J. R. Olson, R. O. Pohl, J. W. Vandersande, A. Zoltan, T. R. Anthony, and W. F. Banholzer, Phys. Rev. B **47**, 14 850 (1993).

⁷L. Wei, P. K. Kuo, R. L. Thomas, T. R. Anthony, and W. F. Banholzer, Phys. Rev. Lett. **70**, 3764 (1993).

⁸M. Asen-Palmer, K. Bartkowski, E. Gmelin, M. Cardona, A. P. Zhernov, A. V. Inyushkin, A. Taldenkov, V. I. Ozhogin, K. M. Itoh, and E. E. Haller, Phys. Rev. B **56**, 9431 (1997).

⁹T. Ruf, R. W. Henn, M. Asen-Palmer, E. Gmelin, M. Cardona, H.-J. Pohl, G. G. Devyatych, and P. G. Sennikov, Solid State Commun. **115**, 243 (2000).

¹⁰R. Berman, *Thermal Conduction in Solids* (Clarendon, Oxford, 1976).

¹¹K. C. Hass, M. A. Tamor, T. R. Anthony, and W. F. Banholzer, Phys. Rev. B **45**, 7171 (1992).

¹²R. Berman, Phys. Rev. B **45**, 5726 (1992).

¹³N. V. Novikov, A. P. Podoba, S. V. Shmegara, A. Witek, A. M. Zaitsev, A. B. Denisenko, W. R. Fahrner, and M. Werner, Diamond Relat. Mater. **8**, 1602 (1999).

¹⁴J. Callaway, Phys. Rev. **113**, 1046 (1959).

¹⁵G. Leibfried and E. Schlömann, Nachr. Akad. Wiss. Göttingen **IIa(4)**, 71 (1954).

¹⁶R. E. Peierls, Ann. Phys. (Leipzig) **3**, 1055 (1929).

¹⁷G. A. Slack and S. Galginitis, Phys. Rev. **133**, A253 (1964).

¹⁸R. O. Pohl, Phys. Rev. **118**, 1499 (1960).

¹⁹B. K. Agrawal and G. S. Verma, Phys. Rev. **128**, 603 (1962).

²⁰R. Berman and J. C. F. Brock, Proc. R. Soc. London, Ser. A **289**, 66 (1965).

²¹R. M. Kimber and S. J. Rogers, J. Phys. C **6**, 2279 (1973).

²²B. Abeles, Phys. Rev. **131**, 1906 (1963).

²³G. A. Slack, Solid State Phys. **34**, 1 (1979).

²⁴J. E. Graebner, M. E. Reiss, L. Seibles, T. M. Hartnett, R. P. Miller, and C. J. Robinson, Phys. Rev. B **50**, 3702 (1994).

²⁵C. H. Xu, C. Z. Wang, C. T. Chan, and K. M. Ho, Phys. Rev. B **43**, 5024 (1991).

²⁶P. G. Klemens, Proc. R. Soc. London, Ser. A **68**, 1113 (1955).

²⁷G. A. Slack (unpublished).

²⁸C. Herring, Phys. Rev. **95**, 954 (1954).

²⁹T. D. Ositinskaya, A. P. Podoba, and S. V. Shmegaera, Sverkhverd. Mater. **14**, 27 (1992).

³⁰C. J. Glassbrenner and G. A. Slack, Phys. Rev. **134**, A1058 (1964).

³¹www.isonics.com

³²J. E. Rapp and H. D. Merchant, J. Appl. Phys. **44**, 3919 (1973).

³³G. Dolling, H. G. Smith, R. M. Nicklow, P. R. Vijayaraghavan, and M. K. Wilkinson, Phys. Rev. **168**, 970 (1968).

³⁴G. Nilsson and G. Nelin, Phys. Rev. B **3**, 364 (1971).

³⁵G. Dolling and R. A. Cowley, Proc. Phys. Soc. London **88**, 463 (1966).

³⁶J. Xie, S. P. Chen, J. S. Tse, S. Gironcoli, and S. Baroni, Phys. Rev. B **60**, 9444 (1999).

³⁷M. Hofmann, A. Zwietz, K. Karch, and F. Bechstedt, Phys. Rev. B **50**, 13 401 (1994).

³⁸G. Kern, G. Kresse, and J. Hafner, Phys. Rev. B **59**, 8551 (1999).

³⁹H. Siegle, G. Kaczmarczyk, L. Filippidis, A. P. Litvinchuk, A. Hoffmann, and C. Thomsen, Phys. Rev. B **55**, 7000 (1997).